Analytical Evaluation of Variables Affecting Surface Wave Testing of Pavements

IGNACIO SANCHEZ-SALINERO, JOSE M. ROESSET, KO-YOUNG SHAO, KENNETH H. STOKOE II, AND GLENN J. RIX

Spectral-Analysis-of-Surface-Waves (SASW) is a promising nondestructive technique for evaluating the mechanical properties of pavement systems and soil deposits. In applying the technique, it is assumed that only plane Rayleigh waves are generated by the source. In reality, when an impulse is applied at the top of a layered system, body waves (shear and compression waves) and other types of surface waves are produced along with Rayleigh waves. In this paper, the dispersion curves (frequency or wavelength versus phase velocity) obtained by assuming only plane Rayleigh waves are compared with dispersion curves obtained when all types of waves are considered. Several cases with different types of layering are studied, and emphasis is placed on typical pavement systems. It is found that the receiver arrangement can significantly influence the dispersion curve and, hence, the resulting modulus profile. For a typical SASW setup in which the distance from the source to the first receiver is kept equal to the distance between the two receivers, wavelengths considered during analysis of the field data should be equal to or less than one-half of the distance between receivers. If this filtering of low frequencies is not performed, the assumption that only plane Rayleigh waves propagate through the medium can lead to errors when backcalculating physical properties from the dispersion curve.

Spectral-Analysis-of-Surface-Waves (SASW) is a nondestructive technique used to evaluate elastic modulus profiles of soil and pavement systems. The method is a modification of the Steady-State-Rayleigh-Wave method that was introduced in the 1950s for measurement of thicknesses and elastic properties of road pavements and soil deposits (*1-6*). Recently the technique has been improved and simplified by the development of digital dynamic signal analyzers (*7-9*).

In the original technique, a steady-state vibrator acting vertically on the surface of the soil or pavement system produced vibrations of a known frequency that propagated along the surface. A vertically oriented sensor (velocity transducer or accelerometer) was moved progressively away from the vibrator and successive positions were found at which surface motions were in phase with the vibrator. The distance between any two of these successive positions corresponds to one wavelength (λ) of the propagating wave. Because the frequency of vibration (f) was known, the velocity of the wave propagating at that frequency could be calculated as

$$V = \lambda \cdot f \tag{1}$$

By repeating this process for different excitation frequencies, a plot of velocity versus frequency (or wavelength) was obtained. Such a plot is known as a dispersion curve.

Most of the energy generated by a vertically acting, surface vibrator is transmitted to the soil or pavement system in the form of Rayleigh waves (surface waves). Body waves (compression and shear waves) are also generated by this source, but, because body waves attenuate more rapidly than the Rayleigh waves near the surface, it is assumed that at large distances from the source the energy carried by the body waves is insignificant compared with that transmitted by the Rayleigh waves. The dispersion curve obtained is therefore assumed to be a curve of phase velocities of Rayleigh waves versus frequency.

The premise underlying the surface wave method is that the propagation velocity of Rayleigh waves is affected primarily by the properties of the upper part of the soil or pavement. The depth of this upper part "sampled" by the waves depends on the frequency of the waves. It is assumed that the bulk of the Rayleigh wave energy travels through a zone about one wavelength deep. By assuming that the velocity obtained at a particular frequency is representative of the properties at a depth of one-half the wavelength, a plot of Rayleigh wave velocities with depth (rather than wavelength) could be obtained. This hypothesis, used in the early stages of the method, is only a rough approximation because the properties of materials above and below a depth of one-half of a wavelength indeed affect the propagation velocity at that frequency. The assumption is, however, fairly good for materials with moduli varying only slightly and smoothly with depth. Shear wave velocity may be obtained from the Rayleigh wave velocity by assuming a Poisson's ratio. The ratio of Rayleigh wave velocity to shear wave velocity varies from 0.874 for a Poisson's ratio of 0.0 to 0.955 for a Poissons's ratio of 0.5. For most practical applications this ratio can be considered equal to 0.92.

I. Sanchez-Salinero, J. M. Roesset, K. H. Stokoe II, and G. J. Rix, Civil Engineering Department, University of Texas at Austin, Austin, Tex. 78712. Current address for Sanchez-Salinero: GEOCISA, Los Llanos de Jerez, 10, Coslada-Madrid, Spain. K.-Y. Shao, Harza Engineering Co., 150 South Wacker Drive, Chicago, Ill. 60606.

If the density (ρ) and Poisson's ratio (ν) of the material are known, the shear modulus (G) and Young's modulus of elasticity (E) can be obtained as

$$G = \rho v_S^2 \tag{2}$$

$$E = 2G(1 + \nu) \tag{3}$$

and a profile of modulus of elasticity versus depth can then be constructed.

The steady-state process is easy to understand and to perform, but field testing can be quite time consuming. In addition, a rigorous inversion process to backcalculate the elastic properties is required for use with pavement systems because the moduli of pavement systems do not vary smoothly with depth.

With the development of digital electronic equipment in the 1970s, the Rayleigh wave procedure regained popularity. Instead of a steady-state vibrator at a fixed frequency, an impulsive or random noise load is applied at the surface of the soil or pavement. Two vertical receivers located on the surface are used to monitor the wave train generated by the source as it passes by them, as shown in Figure 1. The electrical signals produced by the receivers are digitized and recorded by a dynamic signal analyzer. The time signals recorded are transformed to the frequency domain using a fast Fourier transform algorithm, and the phase difference (ϕ) between the two signals is calculated for each frequency. A travel time (t) between receivers can be obtained for each frequency by

$$t = \phi / 2\pi f \tag{4}$$

where the phase difference (ϕ) is in radians and the frequency (f) is in cycles per second. Because the distance between receivers (d) is known, a velocity is calculated as

$$V = d/t \tag{5}$$

Details of the process can be found elsewhere (*7-10*).

One of the advantages of the SASW method with respect to the Steady-State-Surface-Wave method is that substantially less time is required in the field. Because impulsive or random noise signals contain a very broad range of frequencies, all information needed can be obtained simultaneously.

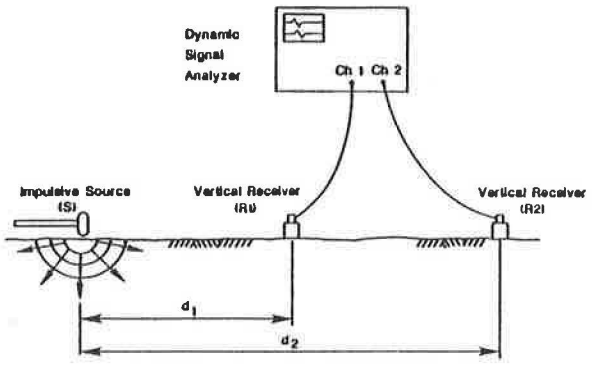

FIGURE 1 Schematic diagram of SASW method.

Another significant improvement of the SASW method is obtained by inverting the dispersion curve. In the inversion process, the elastic properties of the different layers are backcalculated by matching a theoretical dispersion curve to the experimental dispersion curve obtained in the field. An iterative procedure based on forward modeling is given by Nazarian (*10*).

There are still several approximations in the SASW method. That body waves are not considered in the method presents one of the major uncertainties. It is also not clear which arrangement of source and receivers should be used to obtain the best results. To better understand the method, a series of analytical studies that simulate the testing procedure has been performed and is presented herein. The procedures used to calculate plane Rayleigh wave dispersion curves and dispersion curves generated by a point load are presented first. The former method assumes that only Rayleigh waves propagate in the medium whereas the latter method also includes the effect of body waves. Dispersion curves obtained using both methods are then compared. Finally, an alternate method to that suggested by Nazarian (*10*) for backcalculating the elastic properties from a dispersion curve is presented. This alternate method has the advantage of being easily automated.

DISPERSION OF PLANE RAYLEIGH WAVES

The plane Rayleigh wave dispersion curve can be calculated using wave propagation theory. The mathematical model consists of a horizontally layered half-space with properties varying from one layer to another but constant within each layer. The waves are assumed to be propagating in the x-z plane. The differential equations for each layer in terms of displacement potentials can be expressed as

$$\frac{\partial^2 \phi}{\partial t^2} = v_p^2 \left(\frac{\partial^2 \phi}{\partial x^2} + \frac{\partial^2 \phi}{\partial z^2} \right) \tag{6}$$

$$\frac{\partial^2 \psi}{\partial t^2} = v_s^2 \left(\frac{\partial^2 \psi}{\partial x^2} + \frac{\partial^2 \psi}{\partial z^2} \right) \tag{7}$$

where

ϕ and ψ = displacement potentials,

$$v_s^2 = G/\rho, \tag{8}$$

$$v_p^2 = 2G(1 - \nu)/\rho(1 - 2\nu), \tag{9}$$

$G = E/[1(1 + \nu)]$ is the shear modulus of the layer, (10)

ρ = density of the layer, and

ν = Poisson's ratio.

The displacements in the x- and z-directions can be expressed in terms of displacement potentials as

$$u = \frac{\partial \phi}{\partial x} - \frac{\partial \psi}{\partial z}$$, where u is the displacement in the x-direction and (11)

$$w = \frac{\partial \phi}{\partial z} + \frac{\partial \psi}{\partial x}$$, where w is the displacement in the z-direction. (12)

Solutions to Equations 6 and 7 are of the form

$$\phi = (a\, e^{imz} + c\, e^{-imz})\, e^{i(kx-\omega t)} \quad (13)$$

$$\psi = (b\, e^{inz} + d\, e^{-inz})\, e^{i(kx-\omega t)} \quad (14)$$

where ω, k, m, and n are constants satisfying the relations

$$k^2 + m^2 = \omega^2/v_p^2 \quad (15)$$

$$k^2 + n^2 = \omega^2/v_s^2 \quad (16)$$

and where

$i = \sqrt{-1}$
ω = frequency in rad/sec, and
a, b, c, and d = constants of integration.

The quotient of the frequency and the wave number in the x-direction (k) is the phase velocity of the wave in the x-direction:

$$V = \omega/k \quad (17)$$

When the values of m and n are imaginary numbers, Equations 13 and 14 represent waves that propagate in the x-direction and whose amplitude decays in the z-direction. This type of wave is called a Rayleigh wave.

The stresses on a horizontal plane can be expressed in terms of displacements as

$$\tau_{xz} = G\left(\frac{\partial u}{\partial z} + \frac{\partial w}{\partial x}\right) \quad (18)$$

$$\sigma z = 2G\left[\frac{\nu}{1-2\nu}\left(\frac{\partial u}{\partial x} + \frac{\partial w}{\partial z}\right) + \frac{\partial w}{\partial z}\right] \quad (19)$$

By substituting Equations 13 and 14 into Equations 11 and 12 and, subsequently, substituting into Equations 18 and 19, the stresses and displacements at the top of the layer can be expressed in terms of the stresses and displacements at the bottom of the layer after the constants of integration are eliminated. For any layer (j) this relationship can be expressed as

$$\begin{bmatrix} U_h \\ S_h \end{bmatrix}_j = [T]_j \begin{bmatrix} U_o \\ S_o \end{bmatrix}_j \quad (20)$$

where

$$U = \begin{bmatrix} u \\ w \end{bmatrix} \text{ and}$$

$$S = \begin{bmatrix} \tau_{xz} \\ \sigma_z \end{bmatrix}$$

and the subscripts h and o indicate bottom and top of layer, respectively. Matrix $[T]$ is called a transfer or propagator matrix because it gives displacements and stresses at the bottom of the layer in terms of displacements and stresses at the top of the layer. Expressions for the elements of matrix $[T]$ can be found elsewhere (*11, 12*).

The compatibility of displacements and stresses at the interface of any two adjacent layers can be written as

$$\begin{bmatrix} U_h \\ S_h \end{bmatrix}_j = \begin{bmatrix} U_o \\ S_o \end{bmatrix}_{j+1} \quad (21)$$

which substituted in Equation 20 results in

$$\begin{bmatrix} U_o \\ S_o \end{bmatrix}_{j+1} = [T]_j \begin{bmatrix} U_o \\ S_o \end{bmatrix}_j \quad (22)$$

If the process is repeated for all of the layers, a relationship can be obtained between the displacements and stresses at the surface of the layered system and those at any depth:

$$\begin{bmatrix} U_o \\ S_o \end{bmatrix}_{n+1} = [T]_n [T]_{n-1} \cdots [T]_1 \begin{bmatrix} U_o \\ S_o \end{bmatrix}_1 \quad (23)$$

If layer $n + 1$ is considered to be a half-space, an equation relating displacements and stresses at the top of the half-space with the amplitudes of the upward and downward propagating waves in the half-space can be written as

$$\begin{bmatrix} U_o \\ S_o \end{bmatrix}_{n+1} = [H]_{n+1} \begin{bmatrix} A \\ B \\ C \\ D \end{bmatrix}_{n+1} \quad (24)$$

where A and B, and C and D, are proportional to the amplitudes of the waves propagating in the downward and upward directions, respectively, in the half-space.

Substituting Equation 24 into Equation 23 results in

$$\begin{bmatrix} A \\ B \\ C \\ D \end{bmatrix}_{n+1} = \left[\begin{array}{c|c} L_{11} & L_{12} \\ \hline L_{21} & L_{22} \end{array}\right] \begin{bmatrix} U_o \\ S_o \end{bmatrix}_1 \tag{25}$$

where matrix $[L]$ is a 4×4 matrix

$$[L] = [H]^{-1}_{n+1} [T]_n [T]_{n-1} \cdots [T]_1 \tag{26}$$

To obtain the natural modes of vibration, no forces are applied at the top of the layered system ($S_{o_1} = 0$) and no waves are assumed to travel upward in the half-space ($C_{n+1} = D_{n+1} = 0$). This leads to the system of equations

$$\begin{bmatrix} A \\ B \\ 0 \\ 0 \end{bmatrix}_{n+1} = \left[\begin{array}{c|c} L_{11} & L_{12} \\ \hline L_{21} & L_{22} \end{array}\right] \begin{bmatrix} U_o \\ 0 \end{bmatrix}_1 \tag{27}$$

To have other than a trivial solution, the determinant of the submatrix L_{21} must be set equal to zero.

$$|L_{21}| = 0 \tag{28}$$

This equation, called the characteristic equation, relates frequency (ω) with phase velocity (V). At any frequency there may be several values of velocity that satisfy this equation. Each value of velocity corresponds to a different mode of propagation and defines a different dispersion curve. A dispersion curve obtained in the field is a combination of different modes of propagation, but it is usually assumed that for shallow sources the major contribution is provided by the first mode.

This procedure was first explained by Thomson (*11*) and Haskell (*12*) and has been the basis of many studies on wave propagation through layered systems in recent years. An alternate method for computing the modes of propagation and dispersion curves can be obtained by using the layer stiffness matrices suggested by Kausel and Roesset (*13*).

Equation 20 can be rearranged so that forces are given in terms of displacements as

$$\begin{bmatrix} S_o \\ S_h \end{bmatrix}_j = [K]_j \begin{bmatrix} U_o \\ U_h \end{bmatrix}_j \tag{29}$$

where $[K]$ is similar to a stiffness matrix. Expressions for the elements of $[K]$ can be found elsewhere (*13*).

By assembling the stiffness matrices of all of the layers (Equation 29), a global stiffness matrix for the complete layered system can be obtained. This global stiffness matrix relates forces per unit area to the displacements at the interfaces between layers. For the half-space, the stiffness matrix directly relates stresses and displacements at the top surface of the half-space.

To calculate the modes of propagation, the determinant of the global stiffness matrix is set equal to zero. This leads to an equation similar to Equation 28.

When the layered system reduces to a uniform half-space, the characteristic equation becomes

$$(2 - V^2/v_s^2)^2 - 4(1 - V^2/v_s^2)^{1/2}(1 - V^2/v_p^2)^{1/2} = 0 \tag{30}$$

where, in this case, v_s and v_p represent the shear and compression wave velocity of the half-space, respectively. This characteristic equation is independent of frequency, indicating that Rayleigh waves are not dispersive when propagating in a uniform half-space.

Dispersion curves for the cases of a soft layer over a stiffer half-space and a stiff layer over a softer half-space are shown in Figures 2 and 3, respectively. The case of the upper soft layer consists of a 10-ft-thick layer with a shear wave velocity of 700 ft/sec, a Poisson's ratio of 0.25, and a mass density of 4 lb-sec^2/ft^4 ($E = 4.90 \times 10^6$ lb/ft^2) overlying a half-space with a shear wave velocity of 1,565 ft/sec, a Poisson's ratio of 0.25, and a mass density of 4 lb-sec^2/ft^4 ($E = 2.45 \times 10^7$ lb/ft^2). It can be observed (Figure 2) that the phase velocity of the Rayleigh wave (V) starts at a value of 1,439 ft/sec for the very low frequencies and decreases to a value of 644 ft/sec at very high frequencies. The first of these velocities (1,439 ft/sec) corresponds to the velocity of a Rayleigh wave in a uniform half-space with the properties of the half-space of the two-layer system, and the second velocity (644 ft/sec) corresponds to that of a Rayleigh wave propagating in a uniform half-space with the properties of the upper layer.

The case of a stiff layer over a softer half-space (Figure 3) presents some complications. At low frequencies ($f < 10$ Hz in the figure), phase velocity increases as frequency increases.

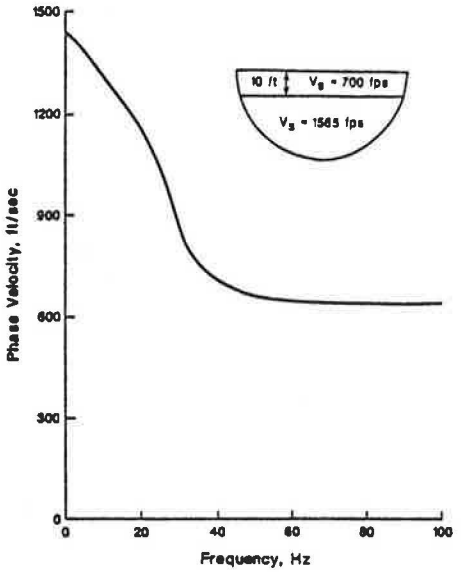

FIGURE 2 Dispersion of plane Rayleigh waves propagating in a layer underlain by a stiffer half-space.

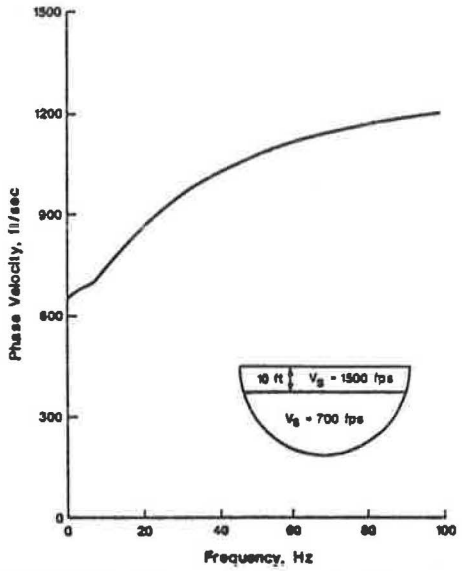

FIGURE 3 Dispersion of plane Rayleigh waves propagating in a layer underlain by a softer half-space.

At some critical frequency ($f \simeq$ 10 Hz in this case) the phase velocity reaches the value of the shear wave velocity in the half-space. For higher frequencies the determinant of Equation 28 becomes complex, and there are no solutions for the phase velocity that satisfy the characteristic equation, indicating that there are no waves of the Rayleigh type (whose amplitude decreases with depth) propagating at frequencies higher than that critical frequency. To obtain a dispersion curve that extends over the entire frequency range, only the real part of the determinant in Equation 28 was considered for the solution of the characteristic equation. The results of this approximation for a layer 10 ft thick with a shear wave velocity of 1,500 ft/sec, a Poisson's ratio of 0.33, and a mass density of 4 lb-sec^2/ft^4 ($E = 2.39 \times 10^7$ lb/ft^2), resting on a half-space with a shear wave velocity of 700 ft/sec, a Poisson's ratio of 0.33, and a density of 4 lb-sec^2/ft^4 ($E = 5.21 \times 10^6$ lb/ft^2), are shown in Figure 3.

DISPERSION CAUSED BY A POINT LOAD

When the SASW technique is used in the field, a transient load is usually applied at a point (or over a small area) on the surface of the pavement or soil deposit. Waves generated by the point load include Rayleigh waves that propagate radially outward from the source along a cylindrical wave front and body waves (shear and compression waves) that propagate outward along a hemispherical wave front. The rate of energy dissipation associated with body waves or the amplitude decrease of body waves is in proportion to the ratio $1/r^2$ along the surface of the layered system, where r is the distance from the source. The amplitude of Rayleigh waves decreases at a rate of $1/r^{1/2}$. In the SASW method it is assumed that because about two-thirds of the energy imparted by the source is transmitted by Rayleigh waves and because these waves attenuate less, the wave train passing by the two receivers is composed primarily of Rayleigh wave components. To study the effect that body wave components might have on the SASW method, dispersion curves caused by a point source were compared with those obtained assuming that only plane Rayleigh waves propagate along the surface.

The formulation used to study the dynamic effects caused by any type of force requires first that the time-history of the specified forces be decomposed into different frequency components (harmonics) using a Fourier series or, more conveniently, a Fourier transform. Results are then obtained for each harmonic and combined via an inverse Fourier transform to obtain the time-history of displacements (Fourier synthesis). For each harmonic (each frequency) the force is expanded in a double Fourier series (or Fourier transform) in the two horizontal directions for cartesian coordinates, or in a Fourier series in the circumferential direction and Hankel transforms in the radial direction for cylindrical coordinates. For each term of these transforms corresponding to a given wave number, the solution can be determined in terms of displacements or stresses by using the global stiffness matrix of the complete layered system as in the approach suggested by Kausel and Roesset (*13*) and outlined in the previous section.

When the solution for each wave number is known, inverse Fourier transforms or Hankel transforms, or both, must be performed to obtain the solution for the specified load distribution. Because the terms of the stiffness matrices of each layer are transcendental functions (complex exponentials), these inverse transforms are very difficult to perform and are done normally by numerical integration. Formulations along these lines have been implemented by Gazetas (*14*) in cartesian coordinates and Apsel (*15*) in cylindrical coordinates. This procedure is particularly convenient when dealing with a uniform half-space or a very small number of layers but extremely expensive when a large number of layers are needed to reproduce the variation of properties with depth.

When the layers are very thin, the transcendental functions representing the variation of displacements with depth can be approximated over each layer by a straight line or any other higher-order polynomial expansion. The solution (displacements and stresses) is then expressed in terms of the exact analytical expression in the two horizontal (or radial and circumferential) directions and in terms of a simpler polynomial expansion in the vertical direction. This approximation leads to much simpler algebraic expressions for the terms of the stiffness matrices of the layers. In addition, when the layered system is underlain by a much stiffer, rocklike material, which can be considered rigid, the wave numbers (eigenvalues) and mode shapes (eigenvectors) of the waves propagating through the layered system can be determined by solving an algebraic eigenvalue problem (*16, 17*). By expressing the solution in terms of these mode shapes (eigenfunction expansion), Kausel (*18*) was able to obtain explicit solutions for the displacements caused by harmonic loads in a layered system. Kausel's formulation is quite efficient from the computational point of view, but the layers must be sufficiently thin to reproduce accurately the variation of the displacements with depth with the linear or higher-order polynomial expansion.

Numerical Implementation

Kausel's formulation was implemented by Shao (*19*) and results from the computer program were compared with those published by Kausel (*18*) with excellent agreement. An approximate formulation for a half-space at the bottom of a layered system was suggested by Hull and Kausel (*20*) and was implemented in the version of the computer program used for the studies presented herein.

Because of the discrete nature of the formulation used, a series of parametric studies was conducted to determine an appropriate mesh size (thickness of the sublayers) to provide an accurate solution. From the results obtained by Shao (*19*) a rule was derived to generate automatically the desired layering. If D is the distance from the point of impact to the point where the displacements are computed, the first depth equal to D is divided into $2N$ sublayers of equal thickness, and the next depth equal to D is divided into N sublayers. N sublayers are then used for the following depth of $2D$, the next depth of $4D$, and so forth. For a nonuniform deposit (such as a pavement) the thickness of each sublayer is the lesser of the value suggested by the rule or the actual physical dimension of the layer. Finally, when the results are to be obtained simultaneously at various points, the smallest value of D controls.

Using this rule, meshes were constructed with values of N equal to 4 (fine mesh), 2 (standard mesh), and 1 (coarse mesh). It was found that the results with the standard mesh were sufficiently accurate for most practical applications. If more accurate results were needed at short distances from the source, a fine mesh was used.

In all cases the thickness of any sublayer should not be greater than 4 to 6 times a reference wavelength. This wavelength can be considered the length of the shear wave in the layer being discretized. Because the wavelength of the shear wave is v_s/f (f being frequency), the maximum thickness of the sublayers varies with each frequency.

Numerical Examples

Dispersion curves were next obtained for a setup similar to that used in the field in an SASW test. The distance from the source to the first receiver was always kept the same as the distance between the two receivers. The load was applied over a circular area with a radius of 1 in. Various frequencies were considered, and for each frequency the distance between the receivers was varied such that the ratio d/λ remained constant. Values of the ratio d/λ (distance divided by the wavelength) of 1/8, 1/4, 1/2, 1, 2, 4, 8, and 16 were used.

A case of a uniform half-space with a shear wave velocity of 700 ft/sec, a density of 4 lb-sec^2/ft^4, and a Poisson's ratio of 0.33 was considered first. The dispersion curves obtained for this case are compared with the one obtained for a plane Rayleigh wave in Figure 4. It can be observed that, at distances from the source of two times the wavelength or more, the dispersion curves for the point load are practically equal to that of a plane Rayleigh wave.

Dispersion curves for the case of a 10-ft-thick soft layer over a stiffer half-space were obtained next. The shear wave velocity of the layer and half-space were 700 and 1,565 ft/sec, respectively. The dispersion curves are shown in Figure 5 and are compared with the dispersion curve obtained for a plane Rayleigh wave. It can be observed that the dispersion curves obtained for distances from the source of two or more times the wavelength are quite similar to that of a plane Rayleigh wave.

Finally, the case of a 10-ft-thick stiff layer (v_s = 1,500 ft/sec) over a softer half-space (v_s = 700 ft/sec) was considered (Figure 6). It is interesting to notice that the dispersion curve

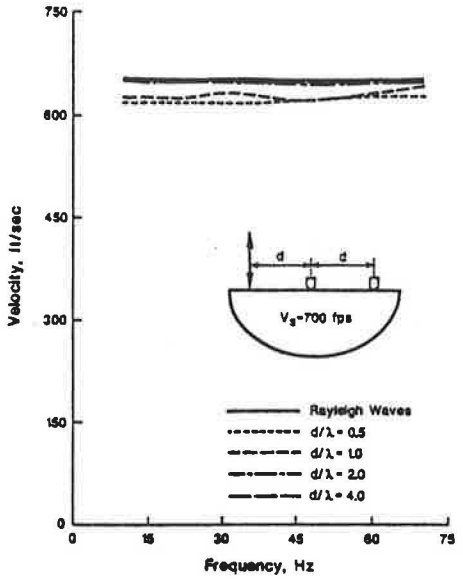

FIGURE 4 Dispersion curves produced by a point load on the surface of a homogeneous half-space compared with the dispersion curve obtained assuming plane Rayleigh waves.

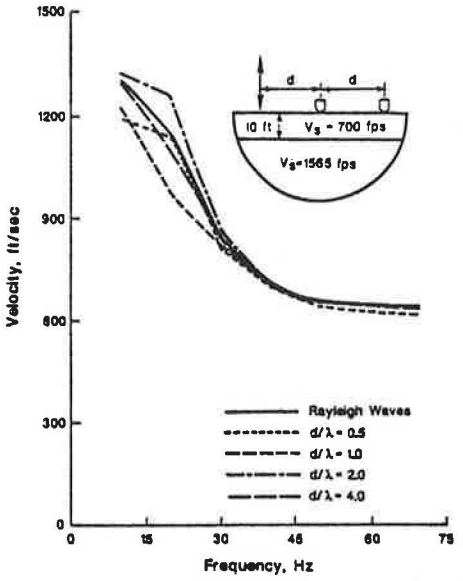

FIGURE 5 Dispersion curves produced by a point load on the surface of a layer underlain by a stiffer half-space compared with the dispersion curve obtained by assuming plane Rayleigh waves.

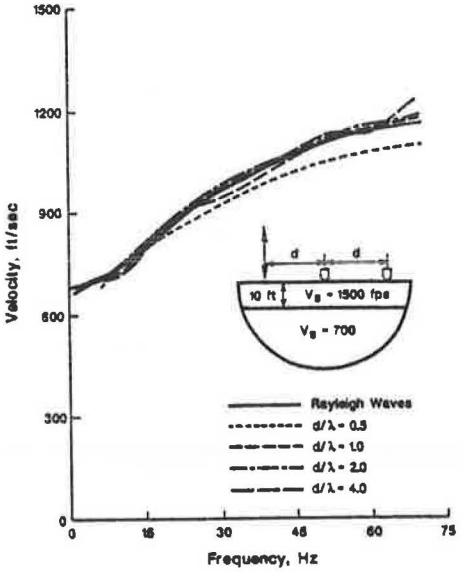

FIGURE 6 Dispersion curves produced by a point load on the surface of a layer underlain by a softer half-space compared with the dispersion curve obtained assuming plane Rayleigh waves.

obtained from the real part of the determinant of Equation 28 for plane Rayleigh waves agrees well with the dispersion curves generated by the point load. At distances from the source of two wavelengths or more the agreement is excellent.

From these comparative studies, it can be concluded that the assumption that only plane Rayleigh waves exist when interpreting the results of an SASW test is best when the distance from the source to the first receiver is of the order of two wavelengths or more.

APPLICATION TO PAVEMENTS

Identification of Mode of Propagation

Application of the SASW method to a three-layer pavement was considered: the first layer (pavement) with a thickness of 2.5 in., a shear wave velocity (v_s) of 1,513 ft/sec, a Poisson's ratio (ν) of 0.35, and a density (ρ) of 4.66 lb-sec^2/ft^4 (modulus of elasticity, $E = 2.88 \times 10^7$ lb/ft^2); the second layer (base) with a thickness of 15 in., V_s = 948 ft/sec, ν = 0.35, and ρ = 4.66 lb-sec^2/ft^4 ($E = 1.13 \times 10^7$ lb/ft^2); and the third layer (subgrade) with v_s = 633 ft/sec, ν = 0.40, and ρ = 3.73 lb-sec^2/ft^4 ($E = 4.18 \times 10^6$ lb/ft^2) and with thickness extending to infinity (a half-space).

The dispersion curve obtained assuming only plane Rayleigh waves is shown in Figure 7 in a semilogarithmic scale. For high frequencies more than one root satisfying the characteristic equation is obtained in the range of phase velocities of interest. It is not immediately apparent which of these roots is the most appropriate.

The dispersion curves resulting from the more accurate analysis, considering a point load at the surface of the pavement, are shown in Figure 8 for various ratios of d/λ (d/λ = 1/4, 1/2, 1, 2, 4), where d is the distance between receivers and λ is the wavelength. It can be observed that the dispersion curves for the different d/λ ratios are nearly identical.

A comparison of the dispersion curves obtained assuming only plane Rayleigh waves with the dispersion curve shown in Figure 8 for d/λ = 4 is shown in Figure 9. The dispersion curve from the point load coincides with the first root of the Rayleigh wave characteristic equation for frequencies below 500 Hz, with the second root for a frequency of 1000 Hz, and with the third root for a frequency of 2000 Hz. To avoid this complication, it was found that if the model for the computation of the Rayleigh wave characteristic equation assumed a uniform half-space beyond a depth of λ, the dispersion curve obtained from the smallest roots of the characteristic equation was the closest to the dispersion curve obtained from the point load at the surface.

Backcalculation of Elastic Properties

When the dispersion curve has been obtained in the field, determination of the elastic moduli requires the solution of an inverse problem. In this work the inversion process adopted consisted of the following steps.

By starting with the results for the highest frequency and assuming a uniform half-space, the apparent wave propagation velocity is assumed to be equal to the Rayleigh wave velocity of the material. Because the results are relatively insensitive to small variations in Poisson's ratio and material density, values of ν = 0.33 and ρ = 3.2 are adopted. It is then possible, from the Rayleigh wave velocity, to compute the shear wave velocity, shear modulus, and Young's modulus of the material.

It is next assumed that these properties, computed assuming only a uniform half-space, are those of a layer with a thickness equal to a factor α times the wavelength λ (values of α of 1/3 to 1 were studied).

By considering the next frequency (second highest) and a profile consisting of a layer with known depth and properties underlain by a half-space, the properties of the half-space that would give a Rayleigh wave velocity equal to the apparent propagation velocity are determined by a search technique. These properties are then assumed to apply from the bottom of the top layer to a depth of $\alpha\lambda$, where λ is the new wavelength.

The procedure is continued, taking successively lower frequencies and proceeding down the profile. At any time, n layers are defined with known thicknesses and material properties and a half-space is assumed to exist below them. The properties of the half-space are determined by a search technique in order to produce a Rayleigh wave velocity equal to the apparent velocity of propagation, and these properties are assumed to apply from the bottom of the nth layer to a depth $\alpha\lambda$.

This first set of computations is quite similar to the direct determination of the dispersion curve for a given profile (a forward problem) and can be performed with relative economy. It should be noticed, however, that when the properties of the underlying half-space have been selected at any step to match the apparent velocity at a given frequency,

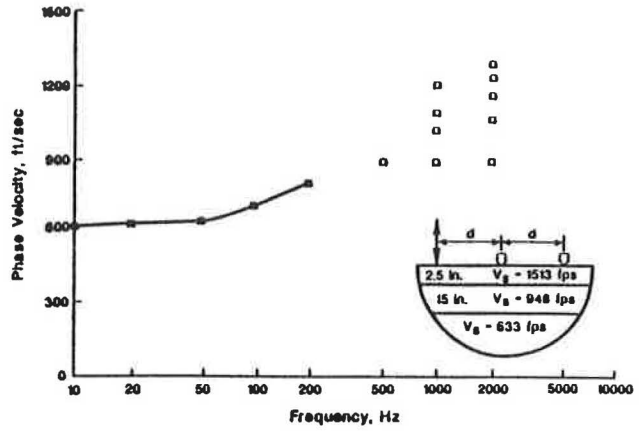

FIGURE 7 Rayleigh wave dispersion of a pavement model.

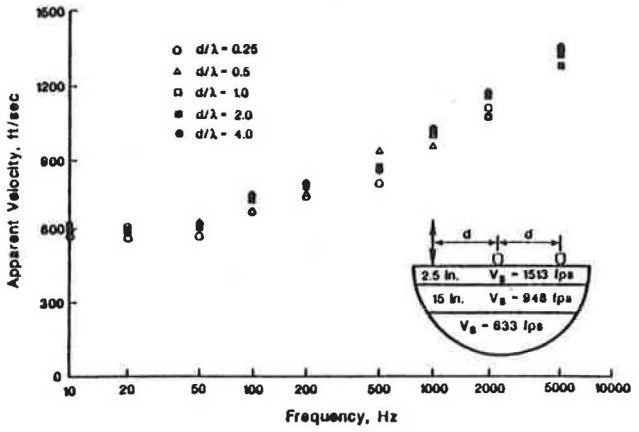

FIGURE 8 Dispersion curves caused by a point load on the surface of a pavement system (obtained with different receiver spacings).

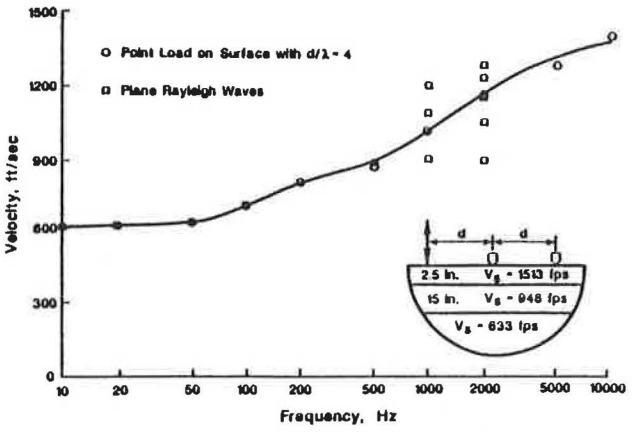

FIGURE 9 Comparison of the dispersion curve produced by a point load on the surface of a pavement with the dispersion curves obtained assuming plane Rayleigh waves.

the resulting profile will no longer match exactly the results at higher frequencies. A correction procedure is therefore necessary. The correction is often performed by considering the complete layered profile obtained after processing all of the frequencies and varying the properties of each layer in order to obtain the best fit.

For pavement systems, if the thicknesses of the layers are known in advance, the correction procedure can be simplified. Only three unknowns (the shear wave velocities of the pavement, base, and subgrade) are considered, and their values are computed using a weighted average of the shear wave velocities of the sublayers contained within the specified layer.

For the case of a half-space, only the first part of the inversion process would be needed. There is no need for correction because the dispersion curve and the properties are independent of frequency and depth. When the suggested inversion program was applied to the results of the uniform half-space studied earlier, a shear wave velocity of 698.7 ft/sec was obtained. The correct result is 700 ft/sec; the difference of 0.2 percent is due to the tolerance in the search technique.

The process was applied next to the dispersion curve calculated for the pavement profile assuming only plane Rayleigh waves. Notice that in this case, because both the computation of the dispersion curve and the inversion procedure are based on the same assumption, comparison of results (original and backcalculated values of the shear wave velocities or elastic moduli) reflects exclusively the errors introduced by the inversion process. Factors influencing the accuracy of the inversion process are the range of frequencies considered, the frequency increment (number of frequencies or points in the dispersion curve), and the value of the parameter α used to define the thickness of the stratum.

Using a maximum frequency of 14 336 Hz, the computed values of the shear wave velocities for the pavement, base, and subgrade estimated with different numbers of points (different frequency increment) are as given in Table 1.

These results were obtained for a value of $\alpha = 1.0$. To get a good approximation of the properties of the pavement, which is very thin, it is necessary to consider very high frequencies. The results improved when higher values were used for the maximum frequency and worsened when lower maximum frequencies were considered.

The results of the inversion process for different values of α (using a maximum frequency of 14 336 Hz and 256 frequencies) are given in Table 2. The agreement appears to be better when using $\alpha = 1$ with maximum errors on the order of 2 percent or less.

To investigate the error in the inversion process created by assuming only a plane Rayleigh wave, the process was applied to the dispersion curves calculated from the more accurate solution of a point load on the surface. This type of dispersion curve should correspond more closely to the values measured experimentally in an SASW test. Notice that in this case the dispersion curve includes the effects of all of the waves generated by the surface load, but the inversion procedure is still based on only plane Rayleigh waves.

The results using the dispersion curve when the two receivers are spaced a distance equal to λ ($d/\lambda = 1$) are given

in Table 3, and those for receivers spaced at a distance 2λ ($d/\lambda = 2$) are given in Table 4.

These results would improve if more frequencies were used. For a distance between receivers of 2λ and a value of $\alpha = 1$, the maximum error is 4 percent (for the shear wave velocity of the base). In all cases the results are generally better for $\alpha = 1$ than for $\alpha = 1/3$.

In practice, the number of frequencies used is normally higher than the number considered in these studies. It is worth noticing that even with $d/\lambda = 1$ and $\alpha = 1/3$ the maximum error, which occurs for the shear wave velocity of the pavement, is only slightly greater than 10 percent. For $\alpha = 1/3$, the estimated shear wave velocities (and therefore the elastic moduli) are always slightly underestimated.

In summary, although the values of α and the distance between receivers affect the results, the errors are relatively small as long as the distance between receivers is of the order of one wavelength or larger and the value of α is between 1/3 and 1. Perhaps the most significant observation is that, in spite of the various approximations, the final results are remarkably consistent.

TABLE 1 COMPUTED VALUES OF SHEAR WAVE VELOCITIES

No. of Frequencies	Δf (Hz)	v_s (ft/sec) of Pavement	Base	Subgrade
64	224	1,508	950	640
128	112	1,509	970	614
256	56	1,509	967	621
512	28	1,509	967	622
Actual value		1,513	948	633

TABLE 2 RESULTS OF INVERSION

α	v_s (ft/sec) of Pavement	Base	Subgrade
1/3	1,385	893	650
1/2	1,444	934	642
1	1,509	967	621
Actual value	1,513	948	633

TABLE 3 RESULTS FOR RECEIVERS SPACED AT $d/\lambda = 1$

α	v_s (ft/sec) of Pavement	Base	Subgrade
1/3	1,351	900	627
1/2	1,432	983	622
1	1,427	1,080	614
Actual value	1,513	948	633

TABLE 4 RESULTS FOR RECEIVERS SPACED AT $d/\lambda = 2$

α	v_s (ft/sec) of Pavement	Base	Subgrade
1/3	1,384	891	634
1/2	1,460	995	628
1	1,514	986	627
Actual value	1,513	948	633

CONCLUSIONS

Interpretation of the results of SASW testing is conducted at present by assuming that only plane Rayleigh waves are generated by the impact. A procedure that accounts for all other types of waves has been presented herein. The conditions under which the assumption that essentially only plane Rayleigh waves are measured during SASW testing is valid were studied. It was found that the distance between receivers relative to the wavelength has a great influence on the results. For a typical SASW setup in which the distance from the source to the first receiver is kept the same as the distance between the two receivers (Figure 1), waves with wavelengths larger than one-half the distance between receivers carry a substantial amount of body wave energy. It is recommended that field data be filtered so that the value of d/λ (distance between receivers over wavelength) is kept greater than 2. A value of 1 could be used if more data were required in the low-frequency range.

A simple procedure for backcalculating properties has also been presented to demonstrate the usefulness of the testing procedure.

REFERENCES

1. R. Jones. A Vibration Method for Measuring the Thickness of Concrete Road Slabs In Situ. *Magazine of Concrete Research,* Vol. 7, No. 20, July 1955.
2. R. Jones. In-Situ Measurement of the Dynamic Properties of Soil by Vibration Methods. *Geotechnique,* Vol. 8, No. 1, March 1958.
3. R. Jones. Surface Wave Technique for Measuring the Elastic Properties and Thickness of Roads: Theoretical Development. *British Journal of Applied Physics,* Vol. 13, 1962.
4. W. Heukelom and C. R. Foster. Dynamic Testing of Pavements. *Journal of the Soil Mechanics and Foundations Division,* ASCE, Vol. 86, No. SM1, Part 1, Feb. 1960.
5. Z. B. Fry. *Development and Evaluation of Soil Bearing Capacity, Foundations of Structures.* Technical Report 3-362, Report 1. U.S. Army Engineer Waterways Experiment Station, Vicksburg, Miss., 1963.
6. R. F. Ballard, Jr. *Determination of Soil Shear Moduli at Depth by In-Situ Vibratory Techniques.* Miscellaneous Paper 4-858. U.S. Army Engineer Waterways Experiment Station, Vicksburg, Miss., Nov. 1964.
7. J. S. Heisey, K. H. Stokoe II, and A. H. Meyer. Moduli of Pavement Systems from Spectral Analysis of Surface Waves. In *Transportation Research Record 852,* TRB, National Research Council, Washington, D.C., 1982, pp. 22-31.

8. S. Nazarian, K. H. Stokoe II, and W. R. Hudson, Use of Spectral Analysis of Surface Waves for Determination of Moduli and Thicknesses of Pavement Systems. In *Transportation Research Record 930,* TRB, National Research Council, Washington, D.C., 1983, pp. 38-46.
9. K. H. Stokoe II and S. Nazarian. Effectiveness of Ground Improvement from Spectral Analysis of Surface Waves. *Proc., Eighth European Conference on Soil Mechanics and Foundation Engineering,* Helsinki, Finland, May 1983.
10. S. Nazarian. *In Situ Determination of Elastic Moduli of Soil Deposits and Pavement Systems by Spectral-Analysis-of-Surface-Waves Method.* Ph.D. dissertation. University of Texas at Austin, Dec. 1984.
11. W. T. Thomson. Transmission of Elastic Waves Through a Stratified Soil Medium. *Journal of Applied Physics,* Vol. 21, Feb. 1950.
12. N. A. Haskell. The Dispersion of Surface Waves on Multilayered Media. *Bulletin of the Seismological Society of America,* Vol. 43, No. 1, Feb. 1953.
13. E. Kausel and J. M. Roesset. Stiffness Matrices for Layered Soils. *Bulletin of the Seismological Society of America,* Vol. 71, No. 6, Dec. 1981.
14. G. Gazetas. *Dynamic Stiffness Functions of Strip and Rectangular Footings on Layered Soil.* S.M. thesis. Massachusetts Institute of Technology, Cambridge, 1975.
15. R. J. Apsel. *Dynamic Green's Functions for Layered Media and Applications to Boundary Value Problems.* Ph.D. dissertation. University of California at San Diego, 1979.
16. G. Waas. *Linear Two Dimensional Analysis of Soil Dynamics Problems on Semi-Infinite Layered Media.* Ph.D. dissertation. University of California, Berkeley, 1972.
17. E. Kausel. *Forced Vibrations of Circular Foundations on Layered Media.* Research Report R74-11. Department of Civil Engineering, Massachusetts Institute of Technology, Cambridge, 1974.
18. E. Kausel. *An Explicit Solution for the Green Functions for Dynamic Loads in Layered Media.* Research Report R81-13. Massachusetts Institute of Technology, Cambridge, 1981.
19. K. Y. Shao. *Dynamic Interpretation of Dynaflect, Falling Weight Deflectometer and Spectral Analysis of Surface Waves Tests on Pavement Systems.* Research Report 437-1. Center for Transportation Research, Bureau of Engineering Research, The University of Texas at Austin, 1986.
20. S. W. Hull and E. Kausel. Dynamic Loads in Layered Half-Space. *Proc., 5th Engineering Mechanics Division Specialty Conference,* ASCE, Laramie, Wyo., 1984.

Publication of this paper sponsored by Committee on Flexible Pavement Design.